Analyst

ROYAL SOCIETY OF CHEMISTRY

PAPER

View Article Online
View Journal | View Issue

Cite this: *Analyst*, 2022, **147**, 2671

A polypyrrole-mediated photothermal biosensor with a temperature and pressure dual readout for the detection of protein biomarkers†

Eunyeong Song,[a] Yingzhou Tao,[b] Haicong Shen,[a] Chaoyong Yang,[a] Tian Tian,*[c] Liu Yang*[a] and Zhi Zhu*[a]

Received 2nd March 2022,
Accepted 25th April 2022

DOI: 10.1039/d2an00370h

rsc.li/analyst

Photothermal biosensors with advantages of speed and high sensitivity offer alternative and reliable solutions for real-time clinical diagnosis, food safety testing and environmental monitoring. Although metallic nanoparticles are usually used for photothermal biosensors, their poor photothermal stability and potential toxicity hinder clinical applications. Taking advantage of the low cytotoxicity and remarkable photothermal effect under the low laser power of polypyrrole-based organic nanoparticles, we developed a novel photothermal biosensor with a temperature and pressure dual readout. After the formation of immunoassay sandwich structures, polypyrrole as the photothermal agent is synthesized *in situ* with pyrrole, HCl and Fe^{3+} released from magnetic Fe_2O_3 particles modified with detection antibody. The heterocyclic rings from polypyrrole enable photothermal performance in the NIR region. The resulting increased heat and pressure in a sealed well are measured using a digital thermometer and a portable pressure meter, respectively. Taking C-reactive protein (CRP) as a model target, the proposed strategy allowed sensitive, selective and accurate analysis of biomarkers, and showed performance comparable to that of ELISA. Overall, the dual-mode photothermal biosensor holds great potential for simple and low-cost photothermal sensing of biomarkers for point-of-care testing (POCT).

Introduction

Clinical diagnosis plays a vital role in helping physicians to choose appropriate treatments for patients with a broad range of diseases. Numerous immunoassays have been developed for sensitive and reliable clinical diagnosis, including the traditional enzyme-linked immunoassay (ELISA),[1] surface-enhanced Raman scattering,[2] chemiluminescence,[3,4] electrochemistry[5] and fluorescence assay.[6,7] According to the report regarding the POCT (point-of-care testing) criteria set forth by the World Health Organization (WHO), the method should be Affordable, Sensitive, Specific, User-friendly, Robust and rapid, Equipment-free and Deliverable (ASSURED).[8] POCT can reduce turnaround times in hospitals, leading to suitable early treatment and enhancing healthcare workflow.[9] Moreover, POCT can be performed in the local setting (home, office, or external field site) at low cost. Regarding POCT applications, the critical bottlenecks of these methods are considered to be the analytical readout methodology. The traditional readout methodology requires spacious analytical equipment and a professionally trained handler, limiting the further potential of widely commercialized POCT applications. Therefore, effective and portable signal transduction systems have been developed, including glucose meters,[10] distance-based chips,[11] thermometers,[12] pressure meters[13] and others.[14]

Thermometers have been widely used in daily life for temperature measurement with the advantages of easy operation, low cost and rapid use.[15–17] Recently, thermometers have also been used for biomolecular detection by reading the temperature increase correlated with target concentration. For example, Gao *et al.* reported that a hydrogel shrinks upon sensing heavy metal ions, leading to capillary flow and release of preloaded NaOH powder into water to increase the temperature.[18] Ma *et al.* used temperature changes caused by the exothermic reaction between H_2O and CaO for target detec-

[a]*MOE Key Laboratory of Spectrochemical Analysis & Instrumentation, The Key Laboratory of Chemical Biology of Fujian Province, State Key Laboratory of Physical Chemistry of Solid Surfaces, Collaborative Innovation Center of Chemistry for Energy Materials, Department of Chemical Engineering, Department of Chemical Biology, College of Chemistry and Chemical Engineering, Xiamen University, Xiamen 361005, China. E-mail: zhuzhi@xmu.edu.cn, yangliu@xmu.edu.cn; Tel: (+86)592-218-7621*
[b]*Integrated Chinese & Western Medicine Oncology Research Center, Jiangxi University of Chinese Medicine, Nanchang, Jiangxi, 330004, China*
[c]*Chemistry and Biomedicine Innovation Center (ChemBIC), School of Chemistry and Chemical Engineering, Nanjing University, Nanjing, 210023, China. E-mail: tiantian@nju.edu.cn*

† Electronic supplementary information (ESI) available. See DOI: https://doi.org/10.1039/d2an00370h

tion.[19] With the photothermal effect, temperature-based measurements can also be realized through light-to-heat signal conversion under laser irradiation because of the localized surface plasmon resonance of nanoparticles.[15,17,20]

The photothermal effect has great potential for POCT because of its superior properties, including simple preparation, low cost, excellent biocompatibility and easy signal readout.[15,16,20–24] A variety of quantitative photothermal immunoassays have been developed using a portable laser pointer as the light source and a thermometer for the signal read-out,[15,22,25] (Table S1†). However, temperature elevation-based detection does not usually produce strong and stable thermal signals. Therefore, it is necessary to explore new photothermal probes and new concise signal readouts to improve the performance and accuracy of photothermal biosensors.

Polypyrrole nanoparticles, as organic photothermal agents, are conductive polymers of pyrrole.[26] They have drawn attention towards biosensing and biomedical applications, owing to their attractive properties of high conductivity, excellent energy conversion efficiency, photothermal stability, and biocompatibility.[27–29] As excellent NIR photothermal probes, polypyrrole nanoparticles have strong light-to-heat energy conversion efficiency with high photothermal stability, due to strong localized surface plasmon resonance absorption in the NIR region.[30] Moreover, polypyrrole does not exhibit photothermal bleaching effects, unlike other photothermal agents whose temperatures decrease under extended laser irradiation even though the temperature consistently increases in the initial stage. With these properties, polypyrrole has been applied in photothermal therapy for tumor ablation[31] as well as biosensors.[32–36] Song *et al.* developed polypyrrole encapsulating iron oxide nanoparticles that absorb the NIR light energy resulting in heat to burn cancer in photothermal therapy.[37] Neither toxicity nor harm to cells was observed.[38–40] Vaitkuviene *et al.* confirmed that polypyrrole below 9.7 μg mL^{-1} did not affect cell viability and proliferation and a low concentration of polypyrrole is biocompatible.[41] Major developments of polypyrrole are employed in the therapy and recently polypyrrole is applied to offer the solutions to medical diagnostic problems. Polypyrrole has been applied in the design of bioanalytical sensors, including catalytic biosensors and electrochemical biosensors. Zhu *et al.* developed a polypyrrole mediated photoelectrochemical immunoassay for the biomarker in heart muscle cells.[42] Yu *et al.* employed a polypyrrole foam-based sensor in immunoassays.[33] To the best of our knowledge, although polypyrrole has become a prominent photothermal agent, there is no report on polypyrrole-mediated photothermal immunoassays using a temperature readout with portable meters for target quantification.

Meanwhile, pressure is another parameter, which has recently been used in sensitive and quantitative immunoassays such as POCT.[13,43–47] In general, pressure sensors have been developed to measure the gas quantity produced by a gas-generating reaction.[47–50] According to the ideal gas approximation ($PV = nRT$), the gas-generating reaction can induce a pressure change related to the change in n, the number of moles of the gaseous reactant or product. Alternatively, if V and n are constant, ΔP (the pressure change between the test system and a control) is proportional to the ΔT (temperature change in kelvins between the control and test). When exposed to light in a specific wavelength range, nanoparticles with a photothermal effect can convert light to heat energy, and further increase the pressure of a sealed system. Therefore, pressure signals can be implemented into photothermal biosensors for a dual readout as mutual references for improved accuracy.

Herein, we developed a simple POCT platform with a thermal and pressure dual readout based on the photothermal effect of polypyrrole. First, a typical sandwich-type immunoassay is performed by capturing the target molecule with an immobilized capture antibody and detection antibody modified with magnetic beads. Then, Fe(III) released from magnetic beads can convert pyrrole into polypyrrole, which then acts as an effective photothermal probe to transform NIR light into heat through the photothermal effect. Finally, the induced temperature and pressure variations are recorded using a digital thermometer and a pressure meter for quantification, respectively. To the best of our knowledge, this is the first attempt to explore a temperature and pressure dual readout-based photothermal immunoassay with polypyrrole as the photothermal probe. The dual-mode photothermal biosensor was applied for the detection of CRP (C-reactive protein), which is one of the responsive protein biomarkers to predict infection, inflammation and risk factors of cardiovascular diseases. Overall, the photothermal platform with a dual readout allows sensitive, selective and accurate analysis of protein biomarkers, for a new POCT with the combined merits of temperature and pressure-based strategies.

Experimental

Reagents and apparatus

CRP proteins, purified mouse monoclonal antibody and biotinylated mouse antibody were obtained from R&D Systems (Minneapolis, MN, USA). Pyrrole, streptavidin-conjugated magnetic beads (Dynabeads M-280, Life Technologies, USA) and IgG (human CD45) were obtained from Life Technologies (Frederick, MD, USA). Tween 20 was obtained from Sangon Biotech (Shanghai, China). Tris-HCl was purchased from Solarbio (Beijing, China). BSA (bovine serum albumin) was purchased from BioFroxx (Einhausen, Germany). HRP-conjugated streptavidin was obtained from Thermo Scientific (Carlsbad, New Mexico, USA). ELISA well strips were obtained from BIOFIL (Beijing, China). The 808 nm portable laser with an output power density of 3 W cm^{-2} was purchased from Guangzhou Yinbeixin Laser Co, LTD (Guangzhou, China). Temperature variation was measured with a digital thermometer (CIE 350P) from CE EMC, Taiwan. The pressure meter was obtained from PASSTECH (Xiamen, China). The UV-vis absorption spectra were recorded with a Spectra Max Id3 system (Molecular Devices, CA, USA). Centrifugation was per-

formed with a Centrifuge-5418 system from Eppendorf (Hamburg, Germany).

Photothermal immunoassay

To monitor the photothermal immunoassay, 4 μg mL^{-1} capture antibody was immobilized in an ELISA well. Different concentrations of the target were dispersed in tubes. Detection antibody-modified magnetic beads (100 μL) and 50 μL of samples were added and incubated at 37 °C for 60 min and gently washed 3 times with washing buffer. An 808 nm laser was used to irradiate each sample with a power density of 0.2 W cm^{-2}, and temperature and pressure changes were measured and recorded using a digital thermometer and a pressure meter, respectively (Fig. S1†), during the laser irradiation. To study the specificity of the polypyrrole mediated photothermal immunoassay, BSA, IgG, Myoglobin (MYO), and Micro-albumin uria (mALB) were measured as control proteins.

Clinical assay with the photothermal immunoassay

To validate the photothermal immunoassay in real samples, human serum samples (5-fold diluted with PBS) spiked with different concentrations of CRP were tested with temperature and pressure changes. Human blood was obtained from Xiamen University Hospital (Xiamen, China) under the approval of the Human Research Ethics Committee (project number: KYX-2018-006). Before use, each blood sample was centrifugated at 2000 rpm for 3 min to remove the precipitate, red blood cells.

Results and discussion

Working principle

The schematic illustration of the working principle is depicted in Fig. 1. The capture antibody is immobilized on a 96-well plate. The biotinylated detection antibody is conjugated to streptavidin magnetic beads through a streptavidin–biotin system *via* streptavidin bridges.[51] With the addition of a CRP target, the target is captured by the immobilized antibody and a sandwiched immunoassay structure is formed by further conjugation with detection antibody-modified magnetic beads. Upon adding the pyrrole substrate, the photothermal probe of polypyrrole is synthesized through pyrrole polymerization with ferric oxide released from the magnetic beads in acidic aqueous solutions. The dark black polypyrrole suspension can be recognized with the naked eye during the polymerization process. Upon irradiation with an 808 nm NIR laser, polypyrrole converts the light excitation energy into thermal energy, resulting in a simultaneous increase in both temperature and pressure in the sealed well, which can be read by a portable thermometer and pressure meter, respectively. With an increase in the concentration of the target protein, more detection antibody-modified magnetic beads are captured. Consequently, more pyrrole polymerization occurs, and thus the temperature and pressure increases are quantitatively proportional to the target concentration.

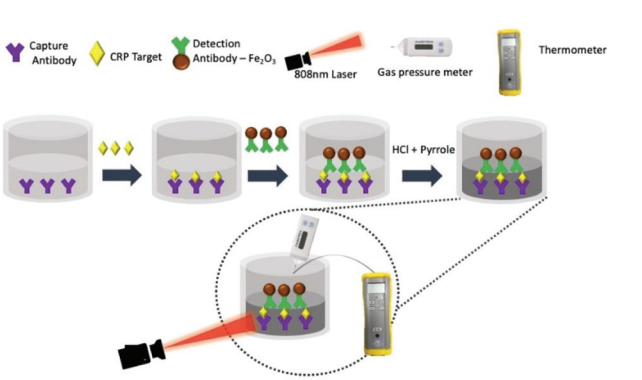

Fig. 1 Schematic illustration of a temperature and pressure-based photothermal biosensor for the detection of CRP with a digital thermometer and a gas pressure meter, respectively.

Feasibility of polypyrrole photothermal performance

The feasibility of the polypyrrole mediated photothermal effect was monitored by adding different components to the photothermal system, and the results are shown in Fig. 2. Pyrrole polymerization is conducted with ferric iron as the oxidizing agent and catalyst. To verify that the photothermal agent polypyrrole was generated from pyrrole, Fe^{3+} and HCl, different combinations of each component, including H_2O, pyrrole, HCl, pyrrole + HCl, Fe^{3+} + HCl, Fe^{3+} + pyrrole, Fe^{3+} and polypyrrole (HCl + Fe^{3+} + pyrrole) were investigated in polymerizations with the same concentrations of 1 M HCl, 0.4 M pyrrole and 3 mM Fe^{3+}. Fig. 2A shows the corresponding UV-Vis spectra for each combination. The black polypyrrole was observed with a wide absorption band from 600 to 900 nm, which was similar to that of the previous report at 400–900 nm,[32] indicating the successful polymerization of pyrrole to polypyrrole. No black color or apparent NIR absorption band was observed for other incomplete component combinations. The strong light absorption band from the charge transfer complex in the NIR region

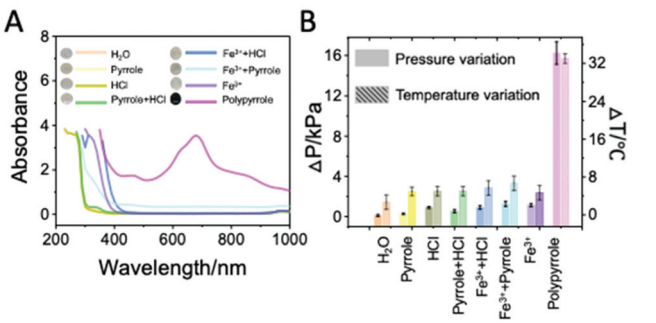

Fig. 2 Feasibility test of the polypyrrole-mediated photothermal biosensor. (A) UV-vis absorption spectra of different components in pyrrole polymerization. Data were captured on the surfaces of each suspension in an ELISA well; (B) temperature and pressure changes of different components after NIR laser irradiation for 5 min with a power density of 0.2 W cm^{-2}. The error bars mean standard deviations from three parallel experiments.

confirmed the possibility of polypyrrole-mediated photothermal performance.

The photothermal performance was further verified by a thermometer or a pressure meter, where different conditions with varied component combinations were tested for temperature or pressure changes under laser irradiation. When exposed to 808 nm laser irradiation for 5 min with a power density of 0.2 W cm^{-2}, the temperature and pressure changes were monitored (Fig. 2B). Polypyrrole sample solutions extraordinarily showed increased temperature and pressure up to 33 °C and 16.5 kPa, respectively, which is attributed to efficient light-to-heat conversion from the broad absorption band in the NIR region.[52]

In contrast, other sample solutions had negligible temperature and pressure variations, indicating that the changes in temperature and pressure were caused by polypyrrole due to the photothermal effect under 808 nm irradiation. In addition, polypyrrole showed excellent repeatable performance over 5 laser on/off cycles (Fig. S2†).

The concentration-dependent effect of Fe^{3+} in pyrrole polymerization was tested (Fig. S3†) and the metal selectivity confirmed that only Fe^{3+} could induce a strong polypyrrole-mediated photothermal effect, while other metal ions commonly existing in biological samples, including Al^{3+}, Na^{+}, K^{+}, Zn^{2+}, and Mg^{2+}, had no effect (Fig. S4†). Overall, polypyrrole can be applied as a photothermal probe for light-to-heat conversion, and the photothermal effect of polypyrrole can be read with not only thermometers but also pressure meters for enhanced accuracy. Theoretically, polypyrrole mediated photothermal biosensors can be used for detecting different kinds of targets.

Quantification of CRP by a polypyrrole-mediated photothermal effect

After optimizing the experimental conditions such as laser power, irradiation time (Fig. S5†) and the HCl concentration (Fig. S6†), CRP quantitative analysis was conducted by measuring both temperature and pressure changes with a digital thermometer and a portable pressure meter, respectively. Monitoring CRP levels with suitable diagnostic accuracy is critical for obtaining early treatment, for example, cardiovascular disease. As shown in Fig. 3A, the temperature gradually increased with an increase in the CRP concentration ranging from 0.75 to 12 mg L^{-1}, where up to 30 °C temperature variation was achieved. In contrast, negligible temperature changes were observed for the control group. The calibration plots in Fig. 3B show a linear relationship between the temperature and CRP concentration in the range of 0.75 to 12 mg L^{-1} with a LOD (Limit of detection) of 0.45 mg L^{-1} based on the definition of the 3σ/slope (σ indicates the standard deviation of blank samples). Meanwhile, the pressure also gradually increased upon increasing the CRP concentration as presented in Fig. 3C, and the pressure increase reached a value of 14.2 kPa at 12 mg L^{-1} CRP. The calibration curve exhibited a good linear correlation between pressure and CRP concentrations in the range of 0.75 to 12 mg L^{-1} with a LOD of 0.31 mg L^{-1} (Fig. 3D). According to the cardiovascular disease

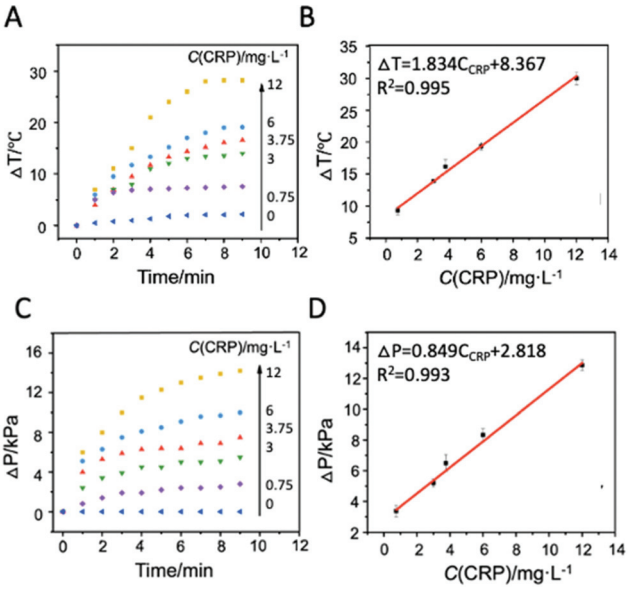

Fig. 3 Sensitivity of the polypyrrole-based photothermal immunoassay for CRP detection. (A) Temperature changes by the thermometer readout; (B) calibration plots of temperature variations; (C) pressure changes by the pressure meter readout; (D) calibration plots of pressure variations. Data were recorded under 808 nm laser irradiation with a power density of 0.2 W cm^{-2} for 9 min. The error bars mean standard deviations from three parallel experiments.

risk levels defined in the standards of the American College of Cardiology,[53] CRP levels are interpreted to consider the disease risk levels where CRP concentrations below 1 mg L^{-1}, within 1 to 3 mg L^{-1} and over 3 mg L^{-1} indicate low, middle and high risks, respectively. Therefore, this temperature and pressure-based photothermal system can satisfy the requirement for disease diagnosis. Moreover, consistency between the concentration-dependent pressure and temperature changes indicates the accuracy of this platform. In addition, it is convenient and economical to employ simple and portable thermometers and pressure meters for detection, while conventional quantitative assays need sophisticated instruments. In brief, this polypyrrole-mediated photothermal immunoassay with a temperature and pressure dual readout can be used in healthcare diagnostics in resource limited regions.

Selectivity is a critical factor for evaluating the photothermal biosensor platform. Hence, common disease biomarkers such as Myoglobin (MYO), urine micro-albumin (mALB) and IgG, as well as control protein BSA, were tested. As shown in Fig. 4, negligible temperature and pressure changes in MYO, mALB, IgG and BSA solutions were observed, while CRP (12 mg L^{-1}) showed a dramatic increase in temperature and pressure, demonstrating the capability of this platform for the selective detection of CRP.

Quantification of CRP in human serum

To verify the potential of the polypyrrole-mediated photothermal biosensor for clinical applications, CRP in human serum was quantified. The serum sample was prepared by centrifu-

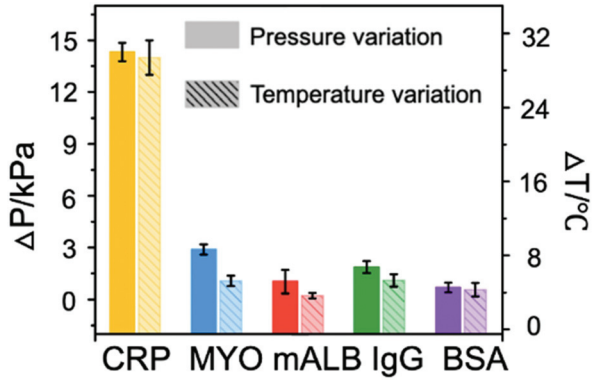

Fig. 4 Selectivity of CRP detection using a polypyrrole mediated photothermal biosensor with temperature and pressure variations. The concentrations of CRP, MYO, mALB, IgG and BSA were 12 mg L^{-1}, 70 μg L^{-1}, 20 mg L^{-1}, 1 g L^{-1} and 50 μg L^{-1}, respectively. The error bars mean standard deviations from three parallel experiments.

gation and was 5-fold pre-diluted using PBS, and then spiked with CRP of different concentrations. Photothermal performance with a power of 0.2 W cm^{-2} under 9 min laser irradiation was tested with a thermometer and pressure meter. As shown in Fig. 5A and B, the calibration curves of temperature and pressure changes with different concentrations of CRP in human serum dilution were established. A linear correlation between temperature and CRP concentration ranging from 0.75–12 mg L^{-1} was obtained, with R^2 = 0.981 and a LOD of 0.75 mg L^{-1}. Meanwhile, a linear correlation between pressure and CRP concentration was also achieved with R^2 = 0.987 and a LOD of 0.41 mg L^{-1}. The LODs of temperature and pressure responses in real samples were comparable to those obtained in buffer, indicating that the polypyrrole mediated photothermal biosensor was hardly affected by the components in real samples, thus holding potential for practical applications.

Furthermore, to validate the precision and credibility of the polypyrrole-mediated photothermal biosensor, the analytical result of CRP (0.75–12 mg L^{-1}) spiked in human serum was compared with that of the standard ELISA method (Fig. S7†). As shown in Fig. 6A and B, both temperature- and pressure-based biosensors showed a good correlation with the ELISA method

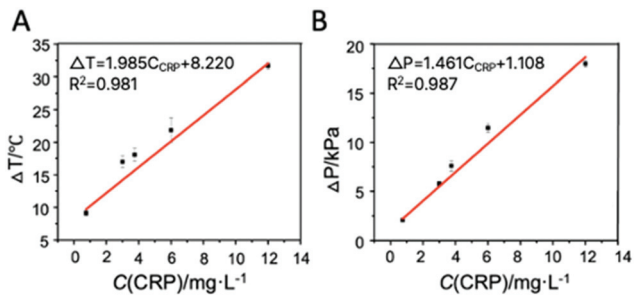

Fig. 5 Photothermal biosensing platform for CRP quantification in human serum: (A) calibration plot of temperature variation; (B) calibration plot of pressure variations.

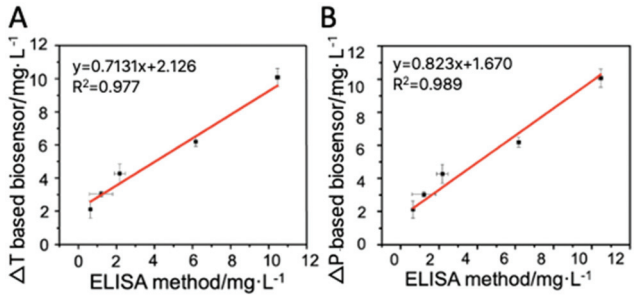

Fig. 6 (A) Validation of the temperature based photothermal biosensor platform by comparing it with ELISA for CRP quantification; and (B) validation of the pressure based photothermal biosensor platform by comparing it with the ELISA method for CRP quantification.

with a correlation coefficient of 0.977 and 0.989, respectively. The results indicate that the accuracy of the proposed photothermal biosensor is comparable to that of the standard method for CRP detection, demonstrating that the developed photothermal biosensor gives sensitive and accurate analysis of biomarkers for clinical diagnosis without additional equipment.

Conclusions

In conclusion, a polypyrrole-mediated photothermal immunoassay was developed with simultaneous temperature and pressure signal transduction. This method takes the following advantages of polypyrrole: (i) easy polymerization with pyrrole and Fe^{3+}, (ii) efficient light-to-heat conversion ensured by strong absorption in the NIR region, (iii) high photothermal stability with reproducibility over 5 times laser on/off irradiation cycles. These characteristics confirm polypyrrole as an excellent photothermal probe, in which temperature and pressure increase are recorded using a simple thermometer and pressure meter, respectively. The developed biosensor was applied for the quantitative assay of CRP with high sensitivity, selectivity and accuracy comparable with those of the standard ELISA approach. Overall, this method provides a user-friendly strategy for the detection of clinical associated biomarkers with dual readouts that can be recorded simply using a thermometer and pressure meter. Furthermore, it contributes to a new research area of photothermal biosensors, promoting the applications of photothermal agents and signal readers in improved photothermal immunoassays such as POCT.

Conflicts of interest

The authors declare no competing financial interest.

Acknowledgements

We thank the National Natural Science Foundation of China (21974113, 21974112, 21927806, 21735004), National Key R&D

Program of China (2021YFA0909400) and the Fundamental Research Funds for the Central Universities (20720210001) for their financial support.

References

1 R. Hu, T. Liu, X.-B. Zhang, Y. Yang, T. Chen, C. Wu, Y. Liu, G. Zhu, S. Huan, T. Fu and W. Tan, *Anal. Chem.*, 2015, **87**, 7746–7753.
2 Z. Rong, C. Wang, J. Wang, D. Wang, R. Xiao and S. Wang, *Biosens. Bioelectron.*, 2016, **84**, 15–21.
3 Y. Chen, J. Sun, Y. Xianyu, B. Yin, Y. Niu, S. Wang, F. Cao, X. Zhang, Y. Wang and X. Jiang, *Nanoscale*, 2016, **8**, 15205–15212.
4 L. Yang, D. Fan, Y. Zhang, C. Ding, D. Wu, Q. Wei and H. Ju, *Anal. Chem.*, 2019, **91**, 7145–7152.
5 H. Li and D. Xu, *TrAC, Trends Anal. Chem.*, 2014, **61**, 67–73.
6 Z. Farka, T. Juřík, D. Kovář, L. Trnková and P. Skládal, *Chem. Rev.*, 2017, **117**, 9973–10042.
7 D. A. Giljohann and C. A. Mirkin, *Nature*, 2009, **462**, 461–464.
8 D. Mabey, R. W. Peeling, A. Ustianowski and M. D. Perkins, *Nat. Rev. Microbiol.*, 2004, **2**, 231–240.
9 J. Park, D. H. Han and J.-K. Park, *Lab Chip*, 2020, **20**, 1191–1203.
10 B. Lin, D. Liu, J. Yan, Z. Qiao, Y. Zhong, J. Yan, Z. Zhu, T. Ji and C. J. Yang, *ACS Appl. Mater. Interfaces*, 2016, **8**, 6890–6897.
11 X. Cui, J. Hu, J. R. Choi, Y. Huang, X. Wang, T. J. Lu and F. Xu, *Anal. Chim. Acta*, 2016, **935**, 207–212.
12 L.-J. Zhi, A.-L. Sun and D. Tang, *Analyst*, 2020, **145**, 4164–4172.
13 B. Lin, Z. Guan, Y. Song, E. Song, Z. Lu, D. Liu, Y. An, Z. Zhu, L. Zhou and C. Yang, *Lab Chip*, 2018, **18**, 965–970.
14 A. Wang, X. Ma, Y. Ye, F. Luo, L. Guo, B. Qiu, Z. Lin and G. Chen, *Anal. Chem.*, 2018, **90**, 1087–1091.
15 G. Fu, S. T. Sanjay, M. Dou and X. Li, *Nanoscale*, 2016, **8**, 5422–5427.
16 X. Han, S. Lin, Y. Li, C. Cheng and X. Han, *Anal. Chim. Acta*, 2020, **1098**, 117–124.
17 W. Zhou, J. Sun and X. Li, *Anal. Chem.*, 2020, **92**, 14830–14837.
18 B. Gao, H. Liu and Z. Gu, *Lab Chip*, 2016, **16**, 525–531.
19 X. Ma, Z. Wang, S. He, C. Chen, F. Luo, L. Guo, B. Qiu, Z. Lin, G. Chen and G. Hong, *ACS Sens.*, 2019, **4**, 2375–2380.
20 G. Fu, S. T. Sanjay, W. Zhou, R. A. Brekken, R. A. Kirken and X. Li, *Anal. Chem.*, 2018, **90**, 5930–5937.
21 M. Luo, X. Xue, H. Rao, H. Wang, X. Liu, X. Zhou, Z. Xue and X. Lu, *Sens. Actuators, B*, 2020, **309**, 127707.
22 S. Du, Y. Wang, Z. Liu, Z. Xu and H. Zhang, *Biosens. Bioelectron.*, 2019, **144**, 111670.
23 G. Fu, Y. Zhu, W. Wang, M. Zhou and X. Li, *ACS Sens.*, 2019, **4**, 2481–2490.
24 G. Fu, Y. Zhu, K. Xu, W. Wang, R. Hou and X. Li, *Anal. Chem.*, 2019, **91**, 13290–13296.
25 S. H. Lee, S. Choi, K. Kwon, N.-H. Bae, B. S. Kwak, W. C. Cho, S. J. Lee and H.-I. Jung, *Sens. Actuators, B*, 2017, **246**, 471–476.
26 K. Deshmukh, M. Basheer Ahamed, R. R. Deshmukh, S. K. Khadheer Pasha, P. R. Bhagat and K. Chidambaram, in *Biopolymer Composites in Electronics*, ed. K. K. Sadasivuni, D. Ponnamma, J. Kim, J. J. Cabibihan and M. A. AlMaadeed, Elsevier, 2017, pp. 27–128. DOI: **10.1016/B978-0-12-809261-3.00003-6**.
27 K. Yang, H. Xu, L. Cheng, C. Sun, J. Wang and Z. Liu, *Adv. Mater.*, 2012, **24**, 5586–5592.
28 Z. Zha, X. Yue, Q. Ren and Z. Dai, *Adv. Mater.*, 2013, **25**, 777–782.
29 J.-Y. Hong, H. Yoon and J. Jang, *Small*, 2010, **6**, 679–686.
30 X. Chen, N. Yu, L. Zhang, Z. Liu, Z. Wang and Z. Chen, *RSC Adv.*, 2015, **5**, 96888–96895.
31 C. Zhang, H. Pan, X. Wang and S.-K. Sun, *Biomater. Sci.*, 2018, **6**, 2750–2756.
32 C. Hong, X. Zhang, C. Wu, Q. Chen, H. Yang, D. Yang, Z. Huang, R. Cai and W. Tan, *ACS Appl. Mater. Interfaces*, 2020, **12**, 54426–54432.
33 Z. Yu, G. Cai, X. Liu and D. Tang, *ACS Appl. Mater. Interfaces*, 2020, **12**, 40133–40140.
34 S. Majumdar, K. Sarmah and D. Mahanta, *ACS Appl. Polym. Mater.*, 2020, **2**, 1933–1942.
35 J. Stejskal, D. Kopecký, H. Kasparyan, J. Vilčáková, J. Prokeš and I. Křivka, *ACS Appl. Nano Mater.*, 2021, **4**, 7513–7519.
36 C. Yang, L. Li, J. Zhao, J. Wang, J. Xie, Y. Cao, M. Xue and C. Lu, *ACS Appl. Mater. Interfaces*, 2018, **10**, 25811–25818.
37 X. Song, H. Gong, S. Yin, L. Cheng, C. Wang, Z. Li, Y. Li, X. Wang, G. Liu and Z. Liu, *Adv. Funct. Mater.*, 2014, **24**, 1194–1201.
38 J. H. Collier, J. P. Camp, T. W. Hudson and C. E. Schmidt, *J. Biomed. Mater. Res.*, 2000, **50**, 574–584.
39 N. Gomez and C. E. Schmidt, *J. Biomed. Mater. Res., Part A*, 2007, **81**, 135–149.
40 J. Y. Lee, C. A. Bashur, A. S. Goldstein and C. E. Schmidt, *Biomaterials*, 2009, **30**, 4325–4335.
41 A. Vaitkuviene, V. Kaseta, J. Voronovic, G. Ramanauskaite, G. Biziuleviciene, A. Ramanaviciene and A. Ramanavicius, *J. Hazard. Mater.*, 2013, **250–251**, 167–174.
42 L.-B. Zhu, L. Lu, H.-Y. Wang, G.-C. Fan, Y. Chen, J.-D. Zhang and W.-W. Zhao, *Biosens. Bioelectron.*, 2019, **140**, 111349.
43 L. Huang, Z. Yu, J. Chen and D. Tang, *ACS Appl. Bio Mater.*, 2020, **3**, 9156–9163.
44 Y. Song, Y. An, W. Liu, W. Hou, X. Li, B. Lin, Z. Zhu, S. Ge, H.-H. Yang and C. Yang, *Chem. Commun.*, 2017, **53**, 11774–11777.
45 Z. Yu, G. Cai, X. Liu and D. Tang, *Anal. Chem.*, 2021, **93**, 2916–2925.
46 J. Hwang, S. G. Lee, S. Kim, J. S. Kim, D. H. Kim and W. H. Lee, *ACS Appl. Polym. Mater.*, 2020, **2**, 2190–2198.

47 D. Liu, S. Jia, H. Zhang, Y. Ma, Z. Guan, J. Li, Z. Zhu, T. Ji and C. J. Yang, *ACS Appl. Mater. Interfaces*, 2017, **9**, 22252–22258.
48 Y. Wang, L. Yang, B. Li, C. J. Yang and Y. Jin, *Anal. Chem.*, 2017, **89**, 8311–8318.
49 P. Biechele, C. Busse, D. Solle, T. Scheper and K. Reardon, *Eng. Life Sci.*, 2015, **15**, 469–488.
50 Z. Yu, Y. Tang, G. Cai, R. Ren and D. Tang, *Anal. Chem.*, 2019, **91**, 1222–1226.
51 M. Wilchek and E. A. Bayer, *Anal. Biochem.*, 1988, **171**, 1–32.
52 D. Jaque, L. Martínez Maestro, B. Del Rosal, P. Haro-Gonzalez, A. Benayas, J. L. Plaza, E. Martín Rodríguez and J. García Solé, *Nanoscale*, 2014, **6**, 9494–9530.
53 D. Liu, F. Liu, Y. Huang, Y. Song, Z. Zhu, S.-F. Zhou and C. Yang, *Analyst*, 2019, **144**, 4188–4193.